

# Photocatalytic degradation of rhodamine B in water by visible light irradiated BMZ nanocomposite

Suranjan Sikdar<sup>1</sup>, Sutanuka Pattanayek<sup>3</sup>, Tanmay K Ghorai<sup>1,2\*</sup>

<sup>1</sup>Department of Chemistry, University of Gour Banga, Malda, West Bengal 732103, India

<sup>2</sup>Department of Chemistry, Indira Gandhi National Tribal University, Amarkantak, Madhya Pradesh 484887, India

<sup>3</sup>Department of Chemistry, West Bengal State University, Barasat, Kolkata, West Bengal 700126, India

\*Corresponding author, Tel: (+91) 35-12223664; Fax: (+91) 35-12223568;

E-mail: tghorai@ugb.ac.in, tanmayghorai66@gmail.com

Received: 31 March 2016, Revised: 28 September 2016 and Accepted: 21 December 2016

DOI: 10.5185/amp.2017/209

www.vbripress.com/amp

## Abstract

The Bi<sub>2</sub>MoZnO<sub>7</sub> nanocomposites have been successfully synthesized via co-precipitation and solid state method and followed by a low temperature calcinations treatment process. We find that such a Bi<sub>2</sub>MoZnO<sub>7</sub> nanocomposite exhibits higher photocatalytic activity and stability than Bi<sub>2</sub>MoO<sub>6</sub>, Bi<sub>2</sub>O<sub>3</sub> and ZnO towards the aqueous phase degradation of Rhodamine B (RhB) under visible light (420 nm < λ). The presence of Bi<sup>3+</sup>/Mo<sup>6+</sup>/Zn<sup>2+</sup> ions in Bi<sub>2</sub>MoZnO<sub>7</sub> and formation of defects in the lattice is believed to play an essential role in affecting the photoreactivity. The different types of active species scavengers are also play the photocatalytic process. The synthesized Bi<sub>2</sub>MoZnO<sub>7</sub> nanocomposites were characterized by UV-Vis spectroscopy, X-ray diffraction (XRD), SEM, TEM, EDAX and IR techniques. The crystallite sizes, particle and grain sizes are 12±2, 5±1 and 100±5 nm, respectively. The rate of degradation of Rhodamine B by BMZ in aqueous phase is 7 times (40.70×10<sup>-3</sup>min<sup>-1</sup>) faster in comparison to pure Bi<sub>2</sub>O<sub>3</sub>/ZnO. Copyright © 2017 VBRI Press.

**Keywords:** Nanocomposite (Bi<sub>2</sub>MoZnO<sub>7</sub>), Bi<sub>2</sub>MoO<sub>6</sub>, ZnO, photocatalytic degradation, rhodamine B, visible light.

## Introduction

Dyes are one of the most notorious contaminants in aquatic environment because of their huge volume of production from industries, slow biodegradation, decoloration and toxicity [1]. Most of the azo dyes are extensively used in textile, paper, leather, gasoline, additives, foodstuffs and cosmetics industry [2]. So it is very much essential to develop methods that can lead to destruction of such hazardous compounds. Removal of coloured contaminants from industrial effluents has been a major concern for waste water treatment. There are so many physical methods [3], biological methods [4-5] and chemical methods [6] are most frequently employed for treatment of remove pollutants from dye industrial effluents. The presence of Rhodamine B, an organic dye in discharged dye effluents is most harmful for human beings [7-9]. The most effective photocatalytic degradation of many dyes was carried out by using nanocomposite semiconductor oxides. Nowadays, different kind of semiconductors has been studied as photocatalyst such as TiO<sub>2</sub>, ZnO, CdS, WO<sub>3</sub>, etc. Most of these semiconductor photocatalysts have band gap equivalent to or larger than 3.2 eV. Therefore, they promote photocatalysis

by irradiated with UV radiation [10-11]. Surface area and surface defects play an important role in the photocatalytic activities of metal oxide nanocomposite. Nanocomposites are ideal candidates for application to photocatalytic degradation of dye since they offer a larger surface-to-volume ratio than nanoparticles. Photo-induced reaction takes place at the surface of the catalyst. A basic mechanism of photocatalytic reaction is on the generation of electron-hole pair and a photocatalyst is illuminated by the light stronger than its band gap energy. The electron migrates from valance band (VB) to conduction band (CB) and holes are formed in the valance band. These holes can generate hydroxyl radicals (·OH) which are highly oxidizing in nature. Probably hole can react with dye molecule and abstract electron from dye molecule and process of degradation start [12-16]. Recently, it has been demonstrated that the semi-conducting materials mediated photocatalytic oxidation reactions of organic compounds are very successful, conventional alternative methods for the removal of organic pollutants from water [17-20]. Among the various photocatalytic semiconducting metal oxide, Zinc oxide (ZnO) is considered to be a technologically prodigious

material having a wide spectrum of applications such as that of a semiconductor ( $E_g = 3.37$  eV), magnetic material, electroluminescent material, UV-absorber, piezoelectric sensor and actuator, nanostructure varistor, field emission displaying material, thermoelectric material, gas sensor, constituent of cosmetics etc [21-23]. The uses of ZnO as a photocatalyst for photodegradation of environmental pollutants has also been extensively studied, because of its nontoxic nature, low cost, and high photochemical reactivity. Bismuth oxide ( $\text{Bi}_2\text{O}_3$ ) has been investigated extensively due to its optical and electrical properties such as refractive index, large energy band gap, dielectric permittivity as well as remarkable photoluminescence and photoconductivity. At the same time molybdenum has also crucial role for his catalytic activity. Therefore, we are very much interested on nanocomposites due to different metal has different properties and gives promising result.

However, here we have been first time reported that the synthesis of  $\text{Bi}_2\text{MoZnO}_7$  nanocomposites by co-precipitation or solid state method. The main focus of this work is to investigate the photo catalytic degradation of Rhodamine B by the use of  $\text{Bi}_2\text{MoZnO}_7$  nanocomposite under visible light. Among the two methods, solid state method is more effective for photocatalytic degradation of RhB. The molecular structure of Rh B and its Zwitterion form are shown in Fig. 1 and Fig. 2.

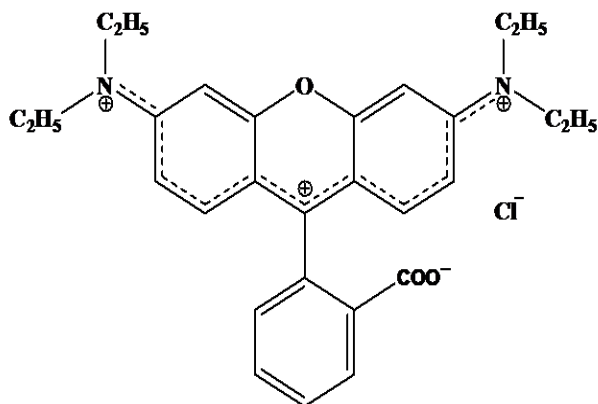


Fig. 1. Structure of Rhodamine B.

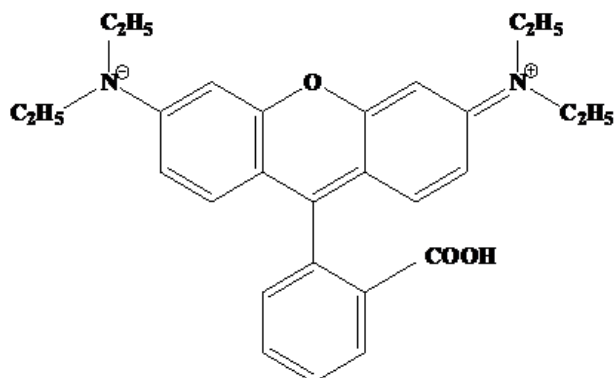


Fig. 2. Zwitterion Structure of Rhodamine B.

## Experimental

### Materials

$\text{NaBiO}_3$  (SDFCL, India),  $(\text{NH}_4)_6\text{Mo}_7\text{O}_{24}\cdot 4\text{H}_2\text{O}$  (SDFCL, India), ZnO (Qualigens Fine Chemicals), dil. HCl (MERCK, India), Conc. $\text{NH}_4\text{OH}$  (MERCK, India), Rhodamine-B (MERCK, India).

### Synthesis of $\text{Bi}_2\text{MoZnO}_7$ nanocomposite by co-precipitation method

The nanocomposite of  $\text{Bi}_2\text{MoZnO}_7$  was prepared by co-precipitation method. The total synthesis was carried out in following steps. In the first step, 1.003 g of  $\text{NaBiO}_3$  was dissolved in 20 mL  $\text{H}_2\text{O}$  and proportionate amount of dil. HCl was added to prepare clear bismuth solution on heating at  $100^\circ\text{C}$  and then added 20 mL EtOH with stirring condition. In the second step 0.1453 g of ZnO was dissolved in  $\text{H}_2\text{O}$  (5 mL) and dilute HCl to prepare Zn solution and dropwise added to Bi- solution. In the third step, 0.3215 g of  $(\text{NH}_4)_6\text{Mo}_7\text{O}_{24}\cdot 4\text{H}_2\text{O}$  of aqueous solution was added and then stirred for an hour at room temperature. After that in stirring condition, conc.  $\text{NH}_4\text{OH}$  was added dropwise to the mixture to adjust the pH of 9.0, a light yellow precipitated was formed. The precipitated was filtered and washed with distilled water several times and dried in a vacuum oven at  $100^\circ\text{C}$  for 2 h and finally obtained the fine powder of  $\text{Bi}_2\text{MoZnO}_7$  nanocomposition. The schematic diagram is following in Flowchart 1 (supplementary file).

### Synthesis of $\text{Bi}_2\text{MoZnO}_7$ nanocomposite by solid state method

The nanocomposite of  $\text{Bi}_2\text{MoZnO}_7$  was also prepared by solid state method. 1.008 gm of  $\text{NaBiO}_3$ , 0.318 gm of  $(\text{NH}_4)_6\text{Mo}_7\text{O}_{24}\cdot 4\text{H}_2\text{O}$  and 0.148 gm of ZnO was taken in the molar ratio 1:2:3 in a porcelain mortar and added acetone drop wise with constant grinding for three hours. A golden yellow solid was obtained and dried it in hot air oven at  $100^\circ\text{C}$  for half an hour.

### Characterization of nanocomposite

The nanocomposite structure of the prepared photocatalysts was measured by X-ray diffractometer (XRD) at room temperature, using a XPERT-PRO PW3071 diffractometer with  $\text{Cu K}\alpha$  ( $\lambda = 1.5418 \text{ \AA}$ ) as target material using 40 kV accelerating voltage, 30 mA emission current. Absorbance of Rhodamine B was measured with the help of UV-VIS spectrophotometer PerkinElmer Lambda 35 (Singapore). The average grain sizes of nanocomposites and atomic level dispersion were measured by scanning electron microscopy (SEM) and energy dispersive X-ray spectroscopy (EDX) (JEOL JMS-5800). FT-IR spectra were recorded at room temperature using a Perkin-Elmer Paragon 1000 FT-IR spectrometer (JEOL JMS-5800). The fine structure of the prepared nanoparticles is analyzed by Transmission Electron Microscopy (TEM) (TM-300, Philips).

### Photocatalytic experiments

The photocatalytic activity of the nanocomposite  $\text{Bi}_2\text{MoZnO}_7$  is substantiated in the following procedure. The photocatalytic reaction was carried out under visible light irradiation. All the experiments were performed at room temperature. Reaction solutions were prepared by adding 0.156gm of photocatalyst nanopowder into 30 ml Rhodamine B (RhB) solution. In this solution, a small volume of the reactant liquid was siphoned out at regular time interval for analysis and the concentration of the dye was measured by absorption spectrometry using UV-vis spectrometer (PERKIN ELMER, LAMBDA 35) at its maximum absorption wavelength of 554nm. The percent of degradation (%) has been calculated as follows:

$$\% \text{ degradation} = (A_0 - A_t) \times 100 / A_0,$$

where,  $A_0$  the initial absorbance and  $A_t$  is the absorbance of the sample irradiated at time,  $t$  minutes.

## Results and discussion

### XRD analysis of nanocomposites

The XRD technique was used to determine and confirm the nanocomposite structure of  $\text{Bi}_2\text{MoZnO}_7$  (BMZ). XRD spectra of  $\text{Bi}_2\text{MoZnO}_7$ ,  $\text{Bi}_2\text{O}_3$  and  $\text{Bi}_2\text{MoO}_6$  are shown in **Fig. 3(a)** in which most of the peaks can be observed at  $2\theta$  values of BMZ are align to  $\text{Bi}_2\text{O}_3$  and  $\text{Bi}_2\text{MoO}_6$  (vertical solid line) at  $12.14^\circ$ ,  $26.26^\circ$ ,  $34.23^\circ$ ,  $40.43^\circ$ ,  $45.59^\circ$ ,  $55.01^\circ$  and  $68.12^\circ$ . The other major distinct peaks are at  $18.26^\circ$ ,  $22.02^\circ$ ,  $32.04^\circ$  and  $41.12^\circ$  may be ZnO. The peak of BMZ is slightly shifting from other compositions due to some oxide defects in the crystals. It clearly indicates that BMZ is a mixture of compositions of all the metal ions. The average crystallite sizes of BMZ,  $\text{Bi}_2\text{O}_3$  and  $\text{Bi}_2\text{MoO}_6$  at  $46.59^\circ$  and  $34.23^\circ$  are  $\sim 12.42$ ,  $\sim 15.25$  and  $15.39\text{nm}$  (calculated from Scherer equation), respectively.

### FT-IR spectra analysis of the BMZ nanocomposites

**Fig. 3(b)** represents the FT-IR spectra of the BMZ,  $\text{Bi}_2\text{O}_3$  and  $\text{Bi}_2\text{MoO}_6$  nanocomposites which are obtained after calcinations for 2 h. It shows that the nanocomposition of BMZ gives absorption peaks at  $3121\text{ cm}^{-1}$  corresponds to the O-H bending mode of vibration is present on the surface due to moisture. The peak appeared at  $1401\text{ cm}^{-1}$  is due to the bending vibration of M-OH groups. The strong band at  $837\text{ cm}^{-1}$  in the infrared spectrum of BMZ is probably arising from stretching modes of Zn-O bands. This spectrum also shows absorption peaks below  $600\text{ cm}^{-1}$  which corresponds to the stretching frequency of Mo=O...Mo bond in BMZ.

### SEM analysis of the BMZ nanocomposites

Scanning electron microscopy is widely used to study the morphological features and surface characteristics of adsorbent materials. **Fig. 4(a)** and **4(b)** indicate the scanning electron microscopy (SEM) at different magnification of  $\text{Bi}_2\text{MoZnO}_7$  performed to gain information about the average grain sizes and surface

morphology of nanocomposition. The SEM images of BMZ confirm that the polymers are flakes in shape and they are arranged in well-ordered manner and average grain sizes are  $\sim 100 \pm 5\text{ nm}$ .

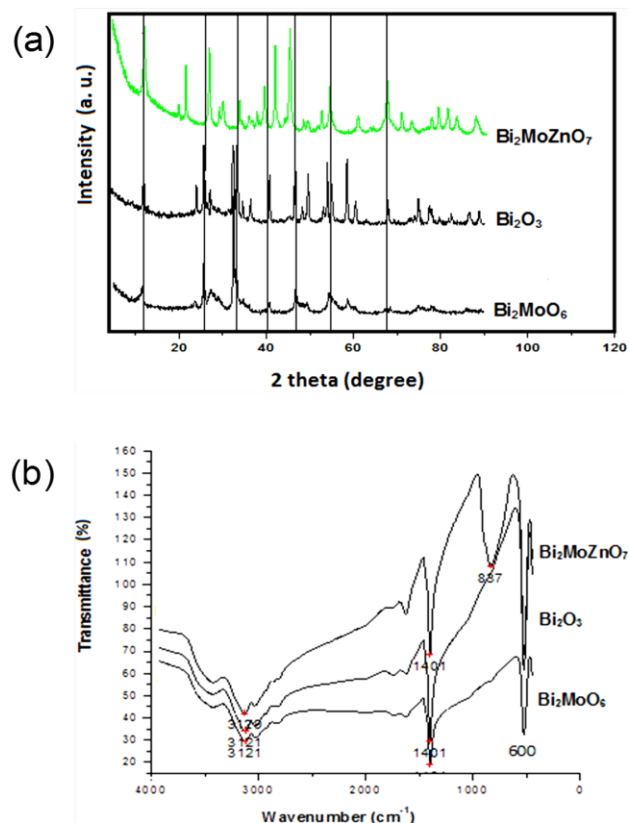


**Fig. 3.** (a) XRD Spectra of  $\text{Bi}_2\text{MoZnO}_7$ ,  $\text{Bi}_2\text{O}_3$  and  $\text{Bi}_2\text{MoO}_6$  nanocomposite and (b) FT-IR spectra of BMZ,  $\text{Bi}_2\text{O}_3$ , and  $\text{Bi}_2\text{MoO}_6$  nanocomposite.

### Energy dispersive X-ray (EDX) spectra analysis of the BMZ nanocomposite

The elemental description of the BMZ was obtained from energy dispersive X-ray analysis. In **Fig. 5**, the peaks located between 2-4, 9-16 and 17-20, and 1-2, 8-9 keV are directly related to the characteristic of bismuth, molybdenum and zinc. Absorption peaks of Carbon, Copper and Zinc is also found and its weight% is high due to the composition is not purified or instrumental error. The weight and atomic % of metal ions are shown in table of  $\text{Bi}_2\text{MoZnO}_7$ .

### TEM analysis of the BMZ nanocomposition

Transmission Electron Microscopy (TEM) is a vital characterization tool for directly imaging nanomaterials to obtain quantitative measures of particle size, size distribution and lattice fringes. The particle size and lattice fringes are measured from HRTEM (Model Philips TM-30, Philips Research Laboratories). The bright-field (BF) electron micrograph of the BMZ nanopowder is produced at  $100^\circ\text{C}$  reflect a spherical particle, with average particle sizes of  $5 \pm 1\text{ nm}$  (**Fig. 4(c)**) and the **Fig. 4(d)** represents the lattice fringes of BMZ

nanoparticles that obtained from HRTEM. The particles had been separated by well-defined boundaries, visible and uniformly distributed.

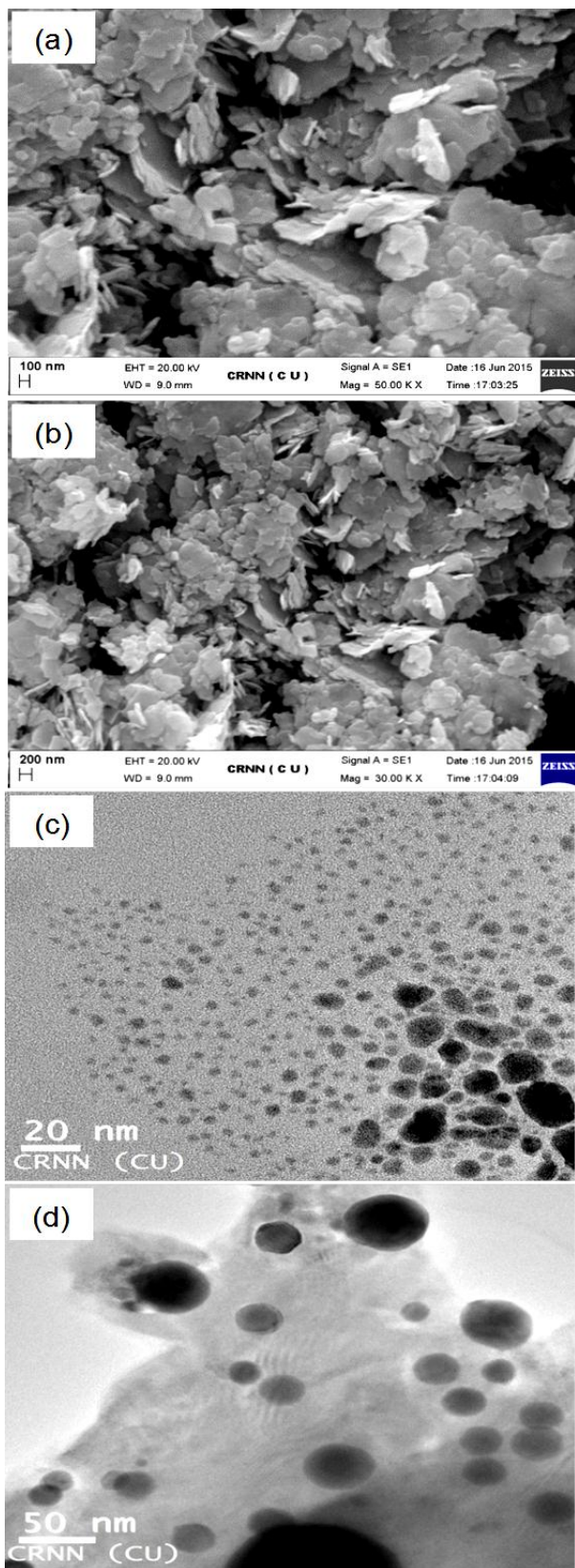


Fig. 4. (a) SEM images of BMZ at 20KV and 50KX magnification; (b) SEM images of BMZ at 20KV and 30KX magnification; (c) TEM image of nanocomposite BMZ; and (d) represent the HRTEM of BMZ.

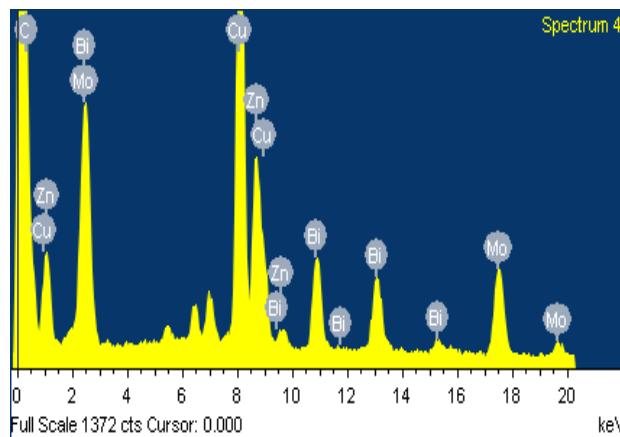


Fig. 5. EDX of BMZ nanocomposition and elemental analysis and determination of Weight% and Atomic% of  $\text{Bi}_2\text{MoZnO}_7$  is shown in table.

Element	Weight (%)	Atomic (%)
C K	7.02	36.02
Cu k	34.56	33.50
Zn K	12.13	11.43
Mo K	15.56	9.99
Bi L	30.73	9.06
Totals	100.00	100.00

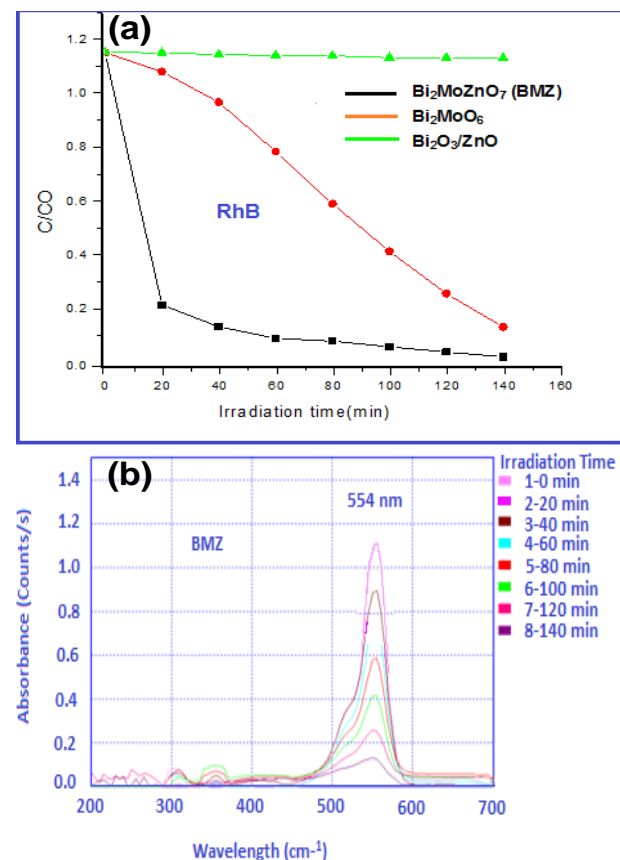


Fig. 6. (a) Degradation of RhB in presence of catalysts BMZ,  $\text{Bi}_2\text{MoO}_6$  and  $\text{Bi}_2\text{O}_3/\text{ZnO}$  under UV light irradiation and (b) the changes in concentration of RhB in presence of BMZ nanocomposite at different irradiation time interval.

### Photocatalytic activity of $\text{Bi}_2\text{MoZnO}_7$ Nanocomposite

The photocatalytic degradation of rhodamine B by  $\text{Bi}_2\text{MoZnO}_7$  (BMZ) was investigated by using a standard UV-Vis spectrophotometer. To study of this reaction, the photocatalyst nanopowder BMZ (0.154 g),  $\text{Bi}_2\text{MoO}_6$  and  $\text{Bi}_2\text{O}_3/\text{ZnO}$  were taken same amount of catalysts in 30 ml rhodamine B into separate beakers. Then a small volume of reactant liquid was siphoned out into a quartz cell and measures the UV-visible spectra in UV-visible spectrophotometer at constant time interval of 20 minutes. It was found that the initial absorption peak of Rh B appears at 554 nm with absorbance of 1.15 which is shown in **Fig. 6(a)**. After addition of the catalyst the pink color of Rh B fades away slowly with the progress of reaction. **Fig. 6(b)** represents the changes in concentration of RhB in presence of BMZ at different irradiation time interval. Among the all catalysts BMZ photocatalyst shows degradation rate 7 times ( $40.70 \times 10^{-3} \text{ min}^{-1}$ ) faster compare the other compositions. The  $\text{Bi}_2\text{O}_3$  or ZnO is almost ineffective for degradation of rhodamine B. The time taken for complete degradation of RhB on BMZ is 140 min shown in **Fig. 6(b)**.

We have study both the compositions of BMZ which are synthesized by co-precipitation and solid state method, the composition obtained by solid state method is slight better photoactive material compared with other method. The rate constant of RhB was measured after 50% decolorization (60 min) shown in **Table 1**. Reaction rate constants were measured after 60 and 140 minutes decolorization of RhB in presence of catalysts and visible light at room temperature.

**Table 1.** Resultant properties of BMZ,  $\text{Bi}_2\text{MoO}_6$  and  $\text{Bi}_2\text{O}_3/\text{ZnO}$  nanocomposites.

Acronym	Crystallites Size (nm)	Degradation rate constant of Rh B k ( $\times 10^{-3} \text{ min}^{-1}$ )		Time required for complete degradation (min) of Rh
		60 (min)	140 (min)	
$\text{Bi}_2\text{MoZnO}_7$ (BMZ)	12.42	40.70	45.38	140
$\text{Bi}_2\text{MoO}_6$	15.39	6.04	14.54	180
$\text{Bi}_2\text{O}_3/\text{ZnO}$	15.25	1.51	1.44	No change

### Conclusion

In summary, we report the facile and green method to synthesize highly stable dispersions of nanocomposite  $\text{Bi}_2\text{MoZnO}_7$  by co-precipitation and solid state method. The various characteristics of the synthesized nanocomposites are analyzed by UV-vis., XRD, EDX and SEM, TEM and IR analyses. The nanocomposite structures were confirmed by XRD. The catalytic activity is investigated by studying the degradation of RhB by BMZ. It shows that the catalytic degradation of RhB with synthesized nanocomposites is much faster in contrast to pure  $\text{Bi}_2\text{MoO}_6$  and  $\text{Bi}_2\text{O}_3/\text{ZnO}$ . The degradation of RhB was found 90% in 150 min by BMZ (co-precipitation method) and it was 98% in 140 min (solid state method).

Since solid state method is relatively simple, fast and environment friendly, this can be scaled up for the bulk production of nanocomposites.

### Acknowledgements

The authors are thankful to the Department of Science and Technology, New Delhi and Department of Chemistry, University of Gour Banga, Malda, W.B. for financial support.

### Author's contributions

Conceived the plan: Tanmay K Ghorai; Performed the experiments: Suranjan Sikdar; Data analysis: S. Sikdar, & T K Ghorai; Wrote the paper: Tanmay K Ghorai, S. Sikdar, (T K Ghorai are the initials of authors); Materials Characterization (TEM, SEM & XRD); Sutanuka Pattanayek. Authors have no competing financial interests.

### Supporting information

Supporting informations are available from VBRI Press.

### References

- Casbeer, E.; Sharm, K, V.; Li, Z,X; *Sep. Purif. Technol.*, **2012**, 87, 1–14.  
DOI: [10.1016/j.seppur.2011.11.034](https://doi.org/10.1016/j.seppur.2011.11.034)
- Straub, F, R.; Voyksner D, R.; Keever, T, J; *Anal. Chem.*, **1993**, 65, 2131–2136.  
DOI: [10.1021/ac00063a034](https://doi.org/10.1021/ac00063a034)
- Guillard, C.; Lachheb,H.; Houas,A.; Ksibi,M.; Elaloui, E.; Herrmann, M-J; *J Photochem. Photobiol. A Chem*, **2003**, 158, 27–36.  
DOI: [10.1016/S1010-6030\(03\)00016-9](https://doi.org/10.1016/S1010-6030(03)00016-9)
- Patil, S., S.; Shinde, M., V.; *Environ. Sci. Technol.*, **1988**, 22, 1160.  
DOI: [10.1021/es00175a005](https://doi.org/10.1021/es00175a005)
- More, T, A.; Vira, A.; Fogel, S; *Environ. Sci. Technol.*, **1989**, 23, 403.  
DOI: [10.1021/es00181a003](https://doi.org/10.1021/es00181a003)
- Yesiladali, S.K.; Pekin, G.; Bermek, H; *World J MicrobiolBiotechnol*, **2006**, 22, 1027.  
DOI: [10.1007/s11274-005-3207-7](https://doi.org/10.1007/s11274-005-3207-7)
- Gupta, K, V.; Khamparia, S.; Tyagi, I. ; Jaspal, D. ; A. Malviya, A; *Global J. Environ. Sci. Manage.*, **2015**, 1, 71-94.  
DOI: [10.7508/gjesm.2015.01.007](https://doi.org/10.7508/gjesm.2015.01.007)
- Ghosh, D.; Bhattacharyya, G, K.; *Appl. Clay Sci.*, **2002**, 20, 295-300.  
DOI: [10.1016/S0169-1317\(01\)00081-3](https://doi.org/10.1016/S0169-1317(01)00081-3)
- Gures ,A.; Karaca ,S.; Dogar ,C.; Bayrak ,R.; Acikyildiz ,M.; Yalcin, M; *J. Colloide Interface Sci.*, **2004**, 269, 310.  
DOI: [10.1016/j.jcis.2003.09.004](https://doi.org/10.1016/j.jcis.2003.09.004)
- Kuo, S.W.; Ho, H, P; *Chemosphere*, **2001**, 45, 77–83.  
DOI: [10.1016/S0045-6535\(01\)00008-X](https://doi.org/10.1016/S0045-6535(01)00008-X)
- Vaidyanathan, S.; Ryan, R, K.; Eduardo, W. E.; *Ind. Eng. Chem. Res.*, **2006**, 45, 2187–2193.  
DOI: [10.1021/ie050693y](https://doi.org/10.1021/ie050693y)
- Kislov, N.; Lahiri, J.; Verma, H.; Yogi Goswami, D.; Stefanakos, E.; Batzill, M; *Langmuir*, **2009**, 25, 3310.  
DOI: [10.1021/ja803845f](https://doi.org/10.1021/ja803845f)
- Baruah, S.; Jaisai, M.; Imani1, R.; Nazhad, M, M.; Dutta, J; *Sci. Technol. Adv. Mater.*, **2010** 11, 7.  
DOI: [10.1088/1468-6996/11/5/055002](https://doi.org/10.1088/1468-6996/11/5/055002)
- Zhu, H.; Jiang, R.; Fu, Y.; Guan, Y.; Yao, J.; Guangming Zeng, X. L.; *Desalination*, **2012**, 286, 41-48.  
DOI: [10.1016/j.desal.2011.10.036](https://doi.org/10.1016/j.desal.2011.10.036)
- Qamar, M.; Muneer, M; *Desalination*, **2009**, 249, 535-540.  
DOI: [10.1016/j.desal.2009.01.022](https://doi.org/10.1016/j.desal.2009.01.022)
- Nirmala, M.; Nair,G, M.; Rekha, K.; Anukaliani, A.; Samdarshi, K,S.; and Nair, G,R.; *African Journal of Basic & App. Sci.*, **2010**, 2, 161-166.  
DOI: [ajbas/ajbas2\(5-6\)106](https://doi.org/10.4236/ajbas.2010.2(5-6)106)
- Houas,A.; Lachheb,H.; Ksibi,M.; Elaloui,E.; Guillard,C.; Herrmann,M-J; *Appl. Catal., B*, **2001**, 31, 145–157.  
DOI: [S0926-3373\(00\)00276-9](https://doi.org/10.1016/S0926-3373(00)00276-9)
- Zhang, F.; Zhao, J.; Shen, T.; Hidaka, H.; Pelizzetti, E.; Serpone, N; *Appl. Catal. B: Environ.*, **1998**, 15, 147.  
DOI: [S0926-3373\(97\)00043-X](https://doi.org/10.1016/S0926-3373(97)00043-X)

19. Wu, G.; Wu, T.; Zhao, J.; H. Hidaka, H.; N. Serpone, N. *Environ. Sci. Technol.* **1999**, 33, 2081.  
**DOI:**[10.1021/es9807643](https://doi.org/10.1021/es9807643)
20. Liu, G.; Li, X.; Zhao, J.; Horikoshi, S.; Hidaka, H.; *J. Mol. Catal. A: Chem.* **2000**, 153, 221  
**DOI:**[10.1016/S1381-1169\(99\)00351-9](https://doi.org/10.1016/S1381-1169(99)00351-9)
21. Prasad, K.; Jha, K, A; *Natural Science*, **2009**, **1**, 129-135.  
**DOI:**[10.4236/ns.2009.12016](https://doi.org/10.4236/ns.2009.12016)
22. Wang, Z, L; (2008). *Nano Res.*, **2008**, 1, 1-8.  
**DOI:**[10.1007/s12274-008-8003-x](https://doi.org/10.1007/s12274-008-8003-x)
23. Méndez, B.; López-Urías, R, A.; Terrones, M. F.; and Terrones, H; (2008). *NanoRes.*, **2008**, 1, 420-426.  
**DOI:** [10.1007/s12274-008-8042-3](https://doi.org/10.1007/s12274-008-8042-3)
24. Zeng, B.; Chen, X.; Ning, X.; Chen, C.; Hu, A.; Deng, W; *Catal. Commun.*, **2014**, 43, 235-239.  
**DOI:**[10.1016/j.catcom.2013.08.003](https://doi.org/10.1016/j.catcom.2013.08.003)